

Spin–orbital interaction for face-sharing octahedra: Realization of a highly symmetric SU(4) model

K. I. Kugel,¹ D. I. Khomskii,² A. O. Sboychakov,¹ and S. V. Streltsov^{3,4}

¹*Institute for Theoretical and Applied Electrodynamics,
Russian Academy of Sciences, Izhorskaya str. 13, 125412 Moscow, Russia*

²*II. Physikalisches Institut, Universität zu Köln, Zùlpicher Str. 77, 50937 Köln, Germany*

³*Institute of Metal Physics, Ural Branch, Russian Academy of Sciences,
S. Kovalevskaya Str. 18, Ekaterinburg, 620990 Russia*

⁴*Ural Federal University, Mira Str. 19, Ekaterinburg, 620002 Russia*

(Dated: January 26, 2022)

Specific features of orbital and spin structure of transition metal compounds in the case of the face-sharing MO₆ octahedra are analyzed. In this geometry, we consider the form of the spin–orbital Hamiltonian for transition metal ions with double (e_g^σ) or triple (t_{2g}) orbital degeneracy. Trigonal distortions typical of the structures with face-sharing octahedra lead to splitting of t_{2g} orbitals into an a_{1g} singlet and e_g^π doublet. For both doublets (e_g^σ and e_g^π), in the case of one electron or hole per site, we arrive at a symmetric model with the orbital and spin interaction of the Heisenberg type and the Hamiltonian of unexpectedly high symmetry: SU(4). Thus, many real materials with this geometry can serve as a testing ground for checking the prediction of this interesting theoretical model. We also compare general trends in spin–orbital (“Kugel–Khomskii”) exchange interaction for three typical situations: those of MO₆ octahedra with common corner, common edge, and the present case of common face, which has not been considered yet.

PACS numbers: 75.25.Dk, 75.30.Et, 75.47.Lx, 71.27.+a, 71.70.Ej, 75.10.Dg

I. INTRODUCTION

Systems with orbital degeneracy usually exhibit quite diverse properties, often much different from those of purely spin systems.^{1–3} In particular, the coupling between orbital and spin degrees of freedom, besides being of practical importance for many specific materials, leads to several interesting theoretical models, such as spin–orbital model (often called the Kugel–Khomskii model)^{4,5}, the popular nowadays compass model^{5,6}, a particular version of which is the renowned Kitaev model.^{6,7}

It turns out that the specific features of one or another system with spin and orbital degeneracy strongly depend on the local geometry. The most typical cases, widely discussed in the literature, are those with MO₆ octahedra (M is a transition metal ion) sharing common oxygen (or common corner), typical e.g. of perovskites like LaMnO₃ or layered systems such as La₂CuO₄, and the situation with two common oxygens for neighboring octahedra (octahedra with common edge), met in many layered systems with triangular lattices such as NaCoO₂ and LiNiO₂. The features of spin–orbital systems in both these cases were studied in detail, see e.g. Refs. 2,8. However, there exists yet the third typical geometry, which is also very often met in many real materials – the case of octahedra with common face (three common oxygens). Strangely enough, this case has not been actually considered in the literature. To fill this gap and to develop a theoretical description of spin–orbital (Kugel–Khomskii) model for this “third case” is the main goal of the present paper.

Interestingly enough, after fulfilling this program, we

have found out that the resulting model has a very symmetric form – more symmetric than for the cases of common corner or common edge. The resulting Hamiltonian in the main approximation turned out to have a very high symmetry: SU(4). Actually, SU(4) model appeared already in the very first treatment of these models^{4,5} for the “artificial” illustrative case, in which for doubly-degenerate orbitals only the diagonal inter-site hopping exists, that is,

$$t_{11} = t_{22} = t, \quad t_{12} = 0, \quad (1)$$

where 1 and 2 are the indices denoting two degenerate orbitals. The resulting exchange Hamiltonian, derived from the degenerate Hubbard model in the strong coupling limit $t/U \ll 1$ (U is the on-site Coulomb repulsion), written in terms of spin $s=1/2$ and pseudospin $\tau=1/2$ operators describing doubly-degenerate orbitals, has a very symmetric form

$$H = \frac{t^2}{U} \sum_{\langle i,j \rangle} \left(\frac{1}{2} + 2\mathbf{s}_i \mathbf{s}_j \right) \left(\frac{1}{2} + 2\boldsymbol{\tau}_i \boldsymbol{\tau}_j \right). \quad (2)$$

This Hamiltonian not only has SU(2)×SU(2) symmetry (it contains scalar products of \mathbf{s} and $\boldsymbol{\tau}$ vector operators), but it shows even much higher SU(4) symmetry (interchange of 4 possible states: $1\uparrow, 1\downarrow, 2\uparrow, 2\downarrow$).

The SU(4) spin–orbital model was extensively discussed in the literature with the main emphasis on novel quantum states (exact solution of the 1D model¹⁰; the presence of three Goldstone modes^{10,11}; the gap formation¹²; spin-orbital singlets on plaquettes in square lattice¹³ and in two-leg ladders¹⁴; spontaneous symmetry breaking with the formation of dimer columns¹⁵; real

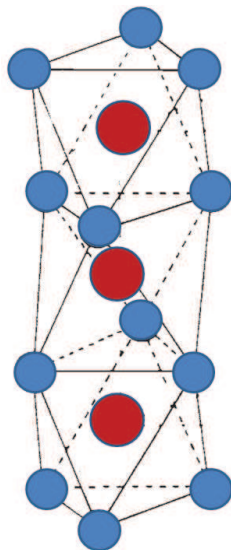


FIG. 1: (Color online) A chain of face-sharing octahedra. Large (red) and small (blue) circles denote metal and ligand ions, respectively.

spin-orbital liquid on honeycomb lattice¹⁶). There were also some attempts to apply this model to real materials.^{9,17–19} Recently the SU(4) model (or more general SU(N) model with N “colors”) has been applied also to cold atoms on a lattice.²⁰ However, especially as to real transition metal compounds, these applications were still rather questionable.^{21,22} In the present paper, we demonstrate that there exists situation in transition metal solids, in which the SU(4) physics might be close to reality – this is the case of spin-orbital systems with face-sharing MO₆ octahedra. If we include the terms in the effective exchange Hamiltonian, which break this SU(4) symmetry, see Appendix C, such terms are usually much weaker than the dominant SU(4) exchange, so that in any case the SU(4) physics would dominate the properties of a system in a broad temperature interval $J' < T < J$, where J is the scale of SU(4) terms in the exchange, and J' – that of symmetry-breaking terms (typically in systems with 3d elements $J' \sim 0.1J$). Even at $T = 0$ strong quantum fluctuations in SU(4) model, especially in one-dimensional systems, may overcome the effect of symmetry-breaking terms.

As far as the actual materials are concerned, in most typical and best studied geometries, such as in systems like perovskites, with corner-sharing MO₆ octahedra and with $\sim 180^\circ$ M–O–M bonds (M is the transition metal), the problem is that conditions (1) required for SU(4) model (2) are not fulfilled. In effect, whereas the spin part of the spin-orbital exchange is of the Heisenberg $\mathbf{s}_i \mathbf{s}_j$ type [SU(2)], the orbital part of the exchange turns out to be very anisotropic, containing terms of the type $\tau^z \tau^z$, $\tau^x \tau^x$, $\tau^y \tau^y$, and also some linear terms, but not, for example $\tau^x \tau^y$. (The latter terms can appear for complex combinations of the basis orbitals, which usually do not lead to static lattice distortions but may be sometime

important giving rise to quite exotic types of the ground state.²³) Also for another well-studied case, that with edge-sharing octahedra and with 90° M–O–M bonds, the situation is more complicated: sometimes the orbital part of the exchange is anisotropic, and in some cases the leading term in the exchange, $\sim t^2/U$, drops out at all and the remaining exchange depends on the Hund’s rule exchange (not included above).^{1,21,24}

The third, much less studied situation, that with the face-sharing MO₆ octahedra (see Fig. 1) is considered below. In situation with face-sharing octahedra, one naturally obtains for the doubly-degenerate case (e_g^σ orbitals, or e_g^π orbitals obtained from triply-degenerate t_{2g} orbitals due to trigonal crystal field, typical for this geometry) that the resulting spin-orbital (Kugel–Khomskii) model is of the type of Eq. (2), i.e. it is the SU(4)-symmetric model. Thus, the systems with this geometry, which are in fact quite abundant among transition metal compounds, represent an actual realization of the high-symmetry SU(4) model, and can provide a natural testing ground for it. The experimental study of the systems with face-sharing arrays may thus allow for verification of the predictions of this model, such as the strong spin-orbital entanglement, and the presence of three Goldstone modes.

Experimentally, there are many transition metal compounds with the face-sharing geometry. Such materials include for example hexagonal crystals like BaCoO₃²⁵, BaVS₃²⁶ or CsCuCl₃²⁷, containing infinite columns of face-sharing ML₆ octahedra (L stands here for ligands O, Cl, S, ...), as shown in Fig. 1. Many other similar systems have finite face-sharing blocks, e.g. BaIrO₃,²⁸ BaRuO₃^{29,30}, or Ba₄Ru₃O₁₀^{31,32} with blocks of three such face-sharing octahedra, connected between themselves by common corners; or blocks of two such octahedra as in large series of systems with general formula A₃(M1)(M2)₂O₉^{33–41}, where A is Ba, Ca, Sr, Li, or Na, and face-sharing M2O₆ octahedra of transition metals are separated by M1O₆ octahedra (which have common corners with M2O₆). Such systems have very diverse properties: some of them are metallic³⁹, others are insulators³² or undergo metal-insulator transition³⁴; despite similar crystal structures they may have charge ordered³⁴ or uniform³⁷ charge states and their magnetic properties are also quite different changing from the singlet ground state^{35,36}, to the situations when part of the magnetic moments turn out to be suppressed^{32,42} and to ferro- or antiferromagnetic order^{25,38,43}. However, in any case, the first problem to consider for such systems is that of a possible orbital and magnetic exchange in this geometry. The analysis of this problem is the main task of the present paper.

In Section II, we formulate a minimal model for the face-sharing geometry, which is in fact the Hubbard model taking into account the orbital degrees of freedom. In Sections III and IV, we consider the chains of face-sharing octahedra with e_g and t_{2g} , respectively, and demonstrate that in both cases we arrive at a highly

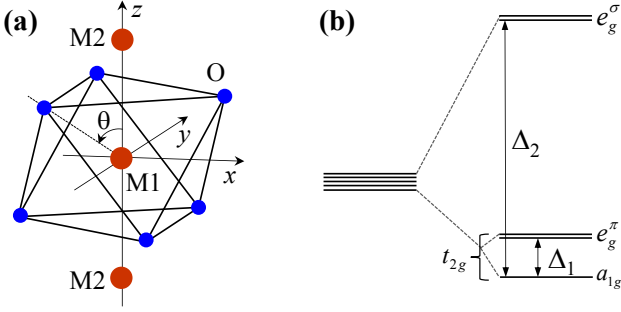


FIG. 2: (Color online) (a) Magnetic atom (M) surrounded by trigonally distorted oxygen (O) octahedron in transition metal compounds with face-sharing octahedra. The global trigonal coordinate is shown. Trigonal distortion is determined by the angle θ ; the value $\cos \theta_0 = 1/\sqrt{3}$ corresponds to undistorted octahedron. Magnetic atoms form a quasi-one-dimensional chain directed along the z axis. (b) Crystal field splitting of d orbitals of the magnetic atom. The splitting of t_{2g} levels (Δ_1) is due to both the trigonal distortions of oxygen octahedra and contribution from neighboring M atoms to the crystal field. The sign of Δ_1 can be different depending on the type of distortions.

symmetrical spin-orbital model. The obtained results are discussed in Section V. More technical issues are discussed in appendices. In Appendix A, we show that trigonal distortions characteristic of the face-sharing geometry do not affect the symmetric form of the effective spin-orbital Hamiltonian. In Appendix B, we derive the explicit form of the electron hopping integrals via ligands as function of an angle characterizing the trigonal distortion of octahedra. In Appendix C, we present the general form of the exchange Hamiltonian including the terms with the Hund's rule coupling, going beyond the symmetric SU(4) form.

II. MODEL

Let us suppose that we have a linear chain of $3d$ magnetic ions. Each of them is located at the center of an octahedron of anions with face-sharing geometry. In contrast to the case of corner-sharing octahedra, where the z direction is usually chosen along the fourfold symmetry axis connecting the transition metal ion with one of the apexes of the ligand octahedron (tetragonal coordinate system), here it is convenient to choose trigonal system with the z axis along the chain and the x and y axes in the plane perpendicular to the chain (see Fig. 2a). In such geometry, two nearest-neighbor ions, M1 and M2, are non-equivalent: a pair ligand triangles surrounding one metal ion can be considered as rotated by 180° with respect to that surrounding another ion.

To formulate a minimal model for the chain, we start from the well-known Hamiltonian in the second quantization that corresponds to a general problem of interacting

electrons

$$H = \sum_{ij} \sum_{\gamma\gamma'\sigma} t_{ij}^{\gamma\gamma'} c_{i\gamma\sigma}^\dagger c_{j\gamma'\sigma} + \frac{1}{2} \sum_i \sum_{\gamma\beta\gamma'\beta'\sigma\sigma'} U_{\gamma\beta;\gamma'\beta'} c_{i\gamma\sigma}^\dagger c_{i\beta\sigma'}^\dagger c_{i\beta'\sigma'} c_{i\gamma'\sigma}. \quad (3)$$

Here, i and j denote lattice sites, where the magnetic ion is located, $\gamma, \gamma', \beta, \beta'$ run over the active orbitals on each site, σ, σ' denote spin up or spin down and $c_{i\gamma\sigma}$, $(c_{i\gamma\sigma}^\dagger)$ are the annihilation (creation) operators for an electron at site i with the quantum numbers γ and σ . The first term describes the kinetic energy and the second one corresponds to the on-site Coulomb repulsion, where

$$U_{\gamma\beta;\gamma'\beta'} = \iint d\mathbf{r} d\mathbf{r}' \phi_\gamma^*(\mathbf{r}) \phi_\beta^*(\mathbf{r}') V(\mathbf{r}, \mathbf{r}') \phi_{\gamma'}(\mathbf{r}) \phi_{\beta'}(\mathbf{r}').$$

Here, $\phi(\mathbf{r})$ are one-particle wave functions and $V(\mathbf{r}, \mathbf{r}')$ describes the interparticle interactions. The crystal field felt by the magnetic ions has an important component of cubic O_h symmetry due to octahedra of anions. It splits the one-electron d levels into a triply degenerate level (t_{2g}) and a doubly degenerate level (e_g). In the case of the face-sharing octahedra, actual symmetry is usually lower than O_h due to, e.g., axial order of the metal ions, which in such a geometry often form chains, dimers, trimers, etc. This type of low-dimensional packing in its turn results in drastic distortions of the ligand octahedra by itself so that octahedra appear to be trigonally distorted (elongation or compression along the vertical z direction in Fig. 2a). Such local distortions of D_{3d} symmetry lead to splitting of t_{2g} orbitals into an a_{1g} singlet and e_g^π doublet; the original e_g (e_g^σ) doublet by that remains unsplit (see below Fig. 2b).

The model treatment will be performed separately for two situations, when e_g and t_{2g} orbitals are active, taking into account trigonal distortions.

III. e_g LEVELS

We first consider the case of one hole (electron) at the degenerate e_g level, which corresponds e.g. to the orbital filling of Cu^{2+} ions in CsCuCl_3 . It has been established (see, e.g. Ref. 44) that both the trigonal field and the spin-orbit coupling do not split the e_g levels.

In the case of ideal MO_6 octahedra, one may use the trigonal coordinate system. The e_g doublet for two neighboring magnetic ions along the chain can be written as⁴⁵

$$\begin{aligned} |d_1\rangle &= \frac{1}{\sqrt{3}} |x^2 - y^2\rangle - \sqrt{\frac{2}{3}} |xz\rangle, \\ |e_1\rangle &= -\frac{1}{\sqrt{3}} |xy\rangle - \sqrt{\frac{2}{3}} |yz\rangle \end{aligned} \quad (4)$$

for an ion M1, and

$$\begin{aligned} |d_2\rangle &= \frac{1}{\sqrt{3}} |x^2 - y^2\rangle + \sqrt{\frac{2}{3}} |xz\rangle, \\ |e_2\rangle &= -\frac{1}{\sqrt{3}} |xy\rangle + \sqrt{\frac{2}{3}} |yz\rangle \end{aligned} \quad (5)$$

for the nearest-neighbor ion M2 (the corresponding structure is illustrated in Fig. 2a).

We start from the two-band 1D Hubbard Hamiltonian of the form of Eq. (3), where orbital indices γ take the values d_1, e_1 for the M1 sites (sites with e.g. odd i) or d_2, e_2 for the M2 sites (sites with even i). We restrict ourselves by the consideration of the nearest neighbor hopping amplitudes along the chain, $t_{\gamma\gamma'} \equiv t_{ii+1}^{\gamma\gamma'}$. These hopping amplitudes have two contributions, which, for this particular geometry, could be of the same order of magnitude; direct hopping between two magnetic ions along the chain, $t_{\gamma\gamma'}^{d-d}$, and the indirect hopping via neighboring anions, $t_{\gamma\gamma'}^{viaA}$. We consider both these situations separately.

We begin by calculating the direct hopping terms. We choose the z direction (trigonal axis) parallel to the chain. In this situation, the only nonzero $d-d$ Slater–Koster parameters⁴⁶ are

$$\begin{aligned} t_{xy,xy} &= t_{x^2-y^2,x^2-y^2} = V_{dd\delta}, \\ t_{yz,yz} &= t_{xz,xz} = V_{dd\pi}. \end{aligned} \quad (6)$$

Therefore, we have for the direct case

$$t^{d-d} \equiv t_{d_2,d_1}^{d-d} = t_{e_2,e_1}^{d-d} = \frac{1}{3}V_{dd\delta} - \frac{2}{3}V_{dd\pi}, \quad (7)$$

and

$$t_{e_2,d_1}^{d-d} = t_{d_2,e_1}^{d-d} = 0. \quad (8)$$

The calculation of effective hoppings via ligands $t_{\gamma\gamma'}^{viaA}$ is more complicated. The direct derivation is performed in Appendix B. Here, we only show that $t_{\gamma\gamma'}^{viaA} \propto \delta_{\gamma\gamma'}$ using simple considerations. Assume that we know hopping integrals along a superexchange path between two neighboring cations involving an anion (A1) located at one of the apexes of the octahedron. In general, we have three nonzero hopping integrals $t_{d_2,d_1}^{viaA1} = t_1$, $t_{e_2,e_1}^{viaA1} = t_2$, and $t_{d_2,e_1}^{viaA1} = t_{e_2,d_1}^{viaA1} = t_3$ between M1 and M2 ions. Then, the hopping integrals for other two superexchange paths (via A2 and A3) could be found by rotating the xy plane by $\pm \frac{2\pi}{3}$ about the trigonal axis. Denoting by primes the axis in the coordinate system rotated by $\frac{2\pi}{3}$, (x', y', z') , $z' = z$, we can write taking into account that $|xy\rangle \propto xy/r^2$ and $|x^2 - y^2\rangle \propto (x^2 - y^2)/(2r^2)$

$$\begin{aligned} |d_i'\rangle &= |d_i'\rangle \cos \frac{2\pi}{3} - |e_i'\rangle \sin \frac{2\pi}{3}, \\ |e_i'\rangle &= |d_i'\rangle \sin \frac{2\pi}{3} + |e_i'\rangle \cos \frac{2\pi}{3}, \end{aligned} \quad (9)$$

where $i = 1, 2$. Therefore

$$\begin{aligned} |d_i'\rangle &= |d_i\rangle \cos \frac{2\pi}{3} + |e_i\rangle \sin \frac{2\pi}{3}, \\ |e_i'\rangle &= -|d_i\rangle \sin \frac{2\pi}{3} + |e_i\rangle \cos \frac{2\pi}{3}. \end{aligned} \quad (10)$$

After the rotation the path M1–A2–M2 becomes the path M1–A1–M2. Thus, we can express the hopping integrals via A2, $t_{d_2,d_1}^{viaA2} = t'_1$, $t_{e_2,e_1}^{viaA2} = t'_2$, and $t_{d_2,e_1}^{viaA2} = t_{e_2,d_1}^{viaA2} = t'_3$ in terms of those via A1 according to $t_{\mu\nu}^{viaA2} = t_{\mu'\nu'}^{viaA1}$. Using Eq. (10), we obtain

$$\begin{aligned} t'_1 &= t_1 \cos^2 \frac{2\pi}{3} + t_2 \sin^2 \frac{2\pi}{3} + t_3 \sin \frac{4\pi}{3}, \\ t'_2 &= t_1 \sin^2 \frac{2\pi}{3} + t_2 \cos^2 \frac{2\pi}{3} - t_3 \sin \frac{4\pi}{3}, \\ t'_3 &= \frac{t_2 - t_1}{2} \sin \frac{4\pi}{3} + t_3 \cos \frac{4\pi}{3}. \end{aligned} \quad (11)$$

The hopping integrals via A3 are found by substituting $\frac{2\pi}{3}$ for $-\frac{2\pi}{3}$:

$$\begin{aligned} t''_1 &= t_1 \cos^2 \frac{2\pi}{3} + t_2 \sin^2 \frac{2\pi}{3} - t_3 \sin \frac{4\pi}{3}, \\ t''_2 &= t_1 \sin^2 \frac{2\pi}{3} + t_2 \cos^2 \frac{2\pi}{3} + t_3 \sin \frac{4\pi}{3}, \\ t''_3 &= \frac{t_1 - t_2}{2} \sin \frac{4\pi}{3} + t_3 \cos \frac{4\pi}{3}. \end{aligned} \quad (12)$$

The total hopping integrals are $t_i^{viaA} = t_i + t'_i + t''_i$ ($i = 1, 2, 3$). Performing the summation over all three paths, we obtain

$$t_{\gamma\gamma'}^{viaA} = t_0 \delta_{\gamma\gamma'}, \quad t_0 = \frac{3}{2}(t_1 + t_2). \quad (13)$$

The value of t_0 as a function of the $p-d$ Slater–Koster parameters $V_{pd\sigma}$ and $V_{pd\pi}$, and the $p-d$ charge transfer energy Δ is calculated in Appendix B. Here, we see that the situation is again similar to the direct exchange, for which we have equal hopping integrals between the same orbitals, and hopping between different orbitals is absent. This is a rather general result based only on the existence of the threefold trigonal axis and it does not depend on the specific features of the superexchange paths. Therefore, the results (7), (8), (13) show that the parameters for the hopping part of the Hamiltonian are $t_{d_2,d_1} = t_{e_2,e_1} = t$ and $t_{e_2,d_1} = t_{d_2,e_1} = 0$ with $t = t^{d-d} + t_0$.

For the Coulomb part of Hamiltonian (3), we can use the standard parametrization: the on-site Coulomb (Hubbard) repulsion on the same orbital $U_{ee,ee} = U_{dd,dd} = U$, and that on different orbitals $U_{de,de} = U' = U - 2J$. Here J is the Hund's rule coupling constant. Note here that the latter relationship is valid only for the unscreened Coulomb potential and can be violated in real transition metal compounds since U is usually screened more by surrounding ligands than the purely intra-atomic parameter J .⁴ In the general case, other Slater integrals,

not only U and J , may enter²; we use below this, the so called Kanamori parametrization, which in most cases is sufficient.

Assuming that $t \ll (U, J)$, we can change over to an effective Hamiltonian that acts on the subspace of functions with singly occupied sites. The calculation is standard (see, e.g., Refs. 4,5). In the first approximation ($J = 0$), the result is the symmetrical SU(4) model

$$H_{eff} = \frac{t^2}{U} \sum_{\langle i,j \rangle} \left(\frac{1}{2} + 2\mathbf{s}_i \mathbf{s}_j \right) \left(\frac{1}{2} + 2\boldsymbol{\tau}_i \boldsymbol{\tau}_j \right), \quad (14)$$

where \mathbf{s}_i is the spin operator of e_g electron at site i defined as $\mathbf{s}_i = \frac{1}{2} \sum_{\gamma\alpha\beta} c_{i\gamma\alpha}^\dagger \boldsymbol{\sigma}_{\alpha\beta} c_{i\gamma\beta}$ and $\boldsymbol{\tau}_i$ is the pseudospin operator for the orbital degree of freedom at site i defined as $\boldsymbol{\tau}_i = \frac{1}{2} \sum_{\alpha\gamma\gamma'} c_{i\gamma\alpha}^\dagger \boldsymbol{\sigma}_{\gamma\gamma'} c_{i\gamma'\alpha}$ ($\boldsymbol{\sigma}$ are the Pauli matrices). Notice that the same $\boldsymbol{\tau}$ operators corresponds to different orbitals at the neighboring sites (since the neighboring face-sharing anion octahedra are rotated with respect to each other). A more general form of the spin-orbital Hamiltonian with the finite Hund's rule coupling J is presented in Appendix C.

Thus, the transition metal compounds with face-sharing octahedra could provide the closest realization of the high-symmetry spin-orbital model. The leading term of the exchange $\sim t^2/U$ has the high SU(4) symmetry, but the terms of higher order containing the Hund's rule coupling constant would have a more complicated form, see Appendix C. The ground state of this general Hamiltonian including terms $\sim J/U$, in the mean-field approximation is well known to be ferromagnetic in spin and antiferromagnetic in pseudospin.^{4,5} In general, however, quantum effects related to the SU(4) symmetry may favor other types of states, and the total resulting type of the ground state requires a special analysis.

The value of the effective electron-electron hopping t depends on the details of the crystal structure, in particular, on the M1–O–M2 angle. Note that at some values of this angle, the contribution of the M1–O–M2 exchange via oxygens can vanish (see Appendix B), and such case should be treated separately.

IV. t_{2g} LEVELS

There are many materials, which have the orbital filling corresponding to the present case. These are not only well-known V_2O_3 and $BaVS_3$, but also many other $3d$ and especially $4d$ and $5d$ transition metal compounds, such as $Ba_4Ru_3O_{10}$ and $BaRuO_3$. As was mentioned above, even in the case of ideal MO_6 octahedra, there exists the trigonal symmetry, which is inherent to face-sharing geometry.

The trigonal crystal field acts on the triplet t_{2g} level further splitting it into a doublet (e_g^π) and a singlet (a_{1g}). The corresponding part of the Hamiltonian due to a trig-

onal field can be written as

$$H_t = \delta \left(L_z^2 - \frac{2}{3} I \right), \quad (15)$$

where I is the unit operator, L_z is the angular momentum operator in the basis of trigonal axes, and parameter δ can be positive or negative. We now analyze the sign of the possible contributions to δ . The trigonal field due to a distortion of the octahedra can have both signs, positive for an elongation and negative for a compression of the octahedra along the trigonal axis. The trigonal field due to the neighboring magnetic cations forming 1D structures is always positive ($\delta > 0$). The singlet is the lowest energy state for $\delta > 0$ and the doublet for $\delta < 0$.

In the trigonal coordinate system, we have the a_{1g} singlet,

$$|a_1\rangle = |3z^2 - r^2\rangle, \quad (16)$$

and a doublet e_g^π ,

$$\begin{aligned} |b_1\rangle &= -\frac{2}{\sqrt{6}}|xy\rangle + \frac{1}{\sqrt{3}}|yz\rangle, \\ |c_1\rangle &= \frac{2}{\sqrt{6}}|x^2 - y^2\rangle + \frac{1}{\sqrt{3}}|xz\rangle, \end{aligned} \quad (17)$$

for an ion M1, and the same singlet

$$|a_2\rangle = |3z^2 - r^2\rangle, \quad (18)$$

and a doublet,

$$\begin{aligned} |b_2\rangle &= -\frac{2}{\sqrt{6}}|xy\rangle - \frac{1}{\sqrt{3}}|yz\rangle, \\ |c_2\rangle &= \frac{2}{\sqrt{6}}|x^2 - y^2\rangle - \frac{1}{\sqrt{3}}|xz\rangle, \end{aligned} \quad (19)$$

for the nearest neighbor ion M2.

It has to be mentioned that these expressions for the wave functions [and Eqs. (4)–(5)] are given for the case of the ideal MO_6 octahedra, where M–O–M angle is about 70.5° . The trigonal distortions will mix e_g^π and e_g^σ orbitals. More detailed calculations, which take into account such modification of the wave function due to trigonal distortions are presented in Appendix A. This mixing, however, only changes some numerical coefficients and does not change the main conclusion that there exist only equal diagonal hoppings, the hopping between different orbitals being zero – the conditions important for getting SU(4) model (14).

Here, we consider the electronic configuration as shown in Fig. 2b: the a_{1g} level has energy lower than that for the e_g^π level. The conditions for the existence of such a configuration are discussed in Appendix A. Further on, we assume that the a_{1g} level is fully occupied, there is one electron at the doubly degenerate e_g^π level, and the upper e_g^σ levels are empty. In this case, we can use 1D two-band Hubbard Hamiltonian in the form of Eq. (3), but now orbital indices γ take the values b_1, c_1 for the

M1 sites (odd i) or b_2, c_2 for the M2 sites (even i). The hopping amplitudes $t_{\gamma\gamma'}$ are the sum of the direct $d-d$ and indirect (via ligands) hopping amplitudes. Note that our analysis is relevant also for the case of negative but large in absolute value Δ_1 , when the empty a_{1g} level lies far above the e_g^π level with one electron.

For the direct $d-d$ hopping, we have now

$$\begin{aligned} t^{d-d} &\equiv t_{b_2, b_1}^{d-d} = t_{c_2, c_1}^{d-d} = \frac{2}{3}V_{dd\delta} - \frac{1}{3}V_{dd\pi}, \\ t_{b_2, c_1}^{d-d} &= t_{c_2, b_1}^{d-d} = 0. \end{aligned} \quad (20)$$

To find the relations for the hopping via ligands, we can use the consideration similar to that used in the previous Section, but with the replacement

$$|d_i\rangle \rightarrow |b_i\rangle, \quad |e_i\rangle \rightarrow |c_i\rangle, \quad i = 1, 2. \quad (21)$$

Repeating after this substitution all calculations as described above, we obtain that the hopping amplitudes have again the symmetric form

$$t_{\gamma\gamma'} = (t^{d-d} + t_0)\delta_{\gamma\gamma'}, \quad (22)$$

where direct hopping amplitude t^{d-d} is given by Eq. (20), while the hopping amplitude via ligands, t_0 , is obtained in Appendix B [Eq. (B7)].

Thus, the same arguments as those presented in the previous section show that for one electron (or hole) at e_g^π levels (neglecting the contribution of a_{1g} states), the effective spin-orbital Hamiltonian for a chain of face-sharing octahedra would have the same form of Eq. (14) as for “real” e_g orbitals, including the SU(4) part, Eq. (14), and if necessary the extra terms^{4,5} $\sim J/U$ (see Appendix C). This form of the effective Hamiltonian is, in fact, a consequence of the lattice symmetry: e_g^π and e_g^σ are similar representations of the same point group. Moreover, taking into account trigonal distortions of the metal-ligand octahedra and the Coulomb interaction between cations in the chain does not change the symmetry of the Hamiltonian (see Appendix A below).

V. CONCLUSIONS

In the present paper, we considered the effective spin-orbital exchange for the “third case” (as compared to the first two well-known cases of MO_6 octahedra with common corner and common edge), namely, the case of local geometry with face-sharing MO_6 octahedra. The trigonal distortions are inherent to such systems. They determine the symmetry of the problem, splitting the t_{2g} levels to those with a_{1g} and e_g^π orbitals and reduce it to appropriate spin-orbital model with pseudospin-1/2. We show that resulting effective spin-orbital Hamiltonian in this situation is a well known symmetric Kugel-Khomskii model, Eq. (2), or, in a more complete form, Eq. (C1), both for the e_g^σ and e_g^π orbitals. The leading terms of the model have the SU(4) symmetry. In that sense, the situation with face-sharing geometry is very different from

the usually considered cases of MO_6 octahedra with a common corner (M1–O–M2 angle $\sim 180^\circ$) and with a common edge (M1–O–M2 angle $\sim 90^\circ$).

This result is important in several respects. First of all, it points out a class of real physical systems, for which the spin-orbital model of SU(4) symmetry can be applied. This opens the possibility to experimentally check some nontrivial predictions of this model, such as strong spin-orbital entanglement and crucial role of quantum effects. Second, it is instructive to compare the general tendencies existing for three typical geometries: those of MO_6 octahedra with a common corner (one common oxygen for two neighboring MO_6 octahedra), common edge (two common oxygens), and a common face (three common oxygens). The general conclusions in the better known first and second cases are rather different. For the common-corner geometry, the typical well-known rule is that the ferro-orbital ordering gives antiferromagnetic spin alignment, and *vice versa*.^{1,2,4,5} However, this is not true for the case of common edges, with $\sim 90^\circ$ M1–O–M2 bonds: in this situation, often one has ferromagnetic spin ordering irrespective of orbital occupation.^{21,24} In that sense, the situation with face-sharing octahedra leading, e.g., to Hamiltonian (14) is more similar to that with a common corner than to the situation with a common edge: ferro-spins coexist with antiferro-orbitals and *vice versa*. On the other hand, as stressed in Appendix B, for the superexchange via ligands (but not for direct $d-d$ hopping!) the leading terms in the exchange $\sim t^2/U \sim [t_{pd}^2/\Delta]^2/U$ can drop out for certain values of the M1–O–M2 angle, similar to the case of common-edge geometry. Thus, the systems with face-sharing geometry represent a class of their own, and they have to be considered as such. Our treatment is focused on the specific features related to such geometry, and the resulting picture turns out to be quite interesting.

Turning to real systems, several factors not considered in the present paper may become important, which could decrease the symmetry of the resulting model. One is the electron-lattice (Jahn–Teller) interaction, which, in principle, could lead to orbital ordering independent of the spin one; in systems like CsCuCl_3 , for example, it could result in helicoidal superstructures (see Ref. 47 and references therein). The second one, considered in detail in the Appendix B, is the strong trigonal distortion of MO_6 octahedra, which for particular situations can strongly reduce the M–O–M contribution to the superexchange, so that for certain M–O–M angle, only the direct $d-d$ contribution remains. In this case, one may need to take into account higher-order terms $\sim J/U$ in the superexchange Hamiltonian. These terms, written down in the general expression (C1) presented in Appendix C, have less symmetric form in orbital variables τ ; i.e., they can also violate the SU(4) symmetry. Nevertheless, pronounced quantum effects typical of the SU(4) model with its intrinsic strong spin-orbital entanglement can still be dominant and determine the type of the ground state of the system. However, even if the

type of the ground state at $T = 0$ would be determined by these symmetry-breaking terms (with the energy scale $J' \sim \frac{t^2}{U} \frac{J}{U}$, which is typically about 10% of the main SU(4) term of the order of $\frac{t^2}{U}$), there would exist a broad temperature range $J' \lesssim T \lesssim \frac{t^2}{U}$, in which the behavior would be determined by the SU(4) physics. However, the situation taking place in each particular real system requires a special treatment.

As far as real materials are concerned, one more issue is worth discussing. Whereas the situation with common corner and common edge geometry is met in all cases, 3D, 2D, and 1D, common-face geometry in this sense is more “choosy”: it is typical for one-dimensional systems (CsCuCl₃, BaCoO₃), and often such face-sharing octahedra exist for just dimers or linear trimers (e.g. in BaIrO₃). We are not aware of any real substances with the 2D or 3D face-sharing geometry, although we cannot exclude such cases in principle. As to the exchange in such hypothetical situations, we can give some arguments that in this case for real e_g systems the resulting Hamiltonian would also be in a first approximation SU(4)-symmetric, but for the t_{2g} levels it would not be the case, because the choice of relevant a_{1g} and e_g^π orbital would depend on the direction and be different for different nearest neighbors. The 1D systems, however, should not necessarily involve straight chains; there may be zigzag or even spiral chains. In all such cases, the SU(4) physics would be preserved for e_g electrons to a first approximation. In some sense, it might be even advantageous, because such 1D model is exactly soluble – although it would be very interesting (if at all possible) to have similar 2D or 3D systems.

Acknowledgments

This work is supported by the Russian Foundation for Basic Research (projects 14-02-00276-a, 14-02-0058-a, 13-02-00050-a, 13-02-00909-a, and 13-02-00374-a), by the Russian Science Support Foundation, by the Ministry of Education and Science of Russia (grant MK 3443.2013.2), by the Ural Branch of Russian Academy of Sciences, by the German projects DFG GR 1484/2-1 and FOR 1346, and by Köln University via the German Excellence Initiative.

Appendix A: Face-sharing octahedra with trigonal distortions

Let us now consider a more general case, namely, that with the crystal field of trigonal symmetry corresponding to the stretching or compression of the chain of face-sharing octahedra. In the main text, we considered exchange interaction for e_g and t_{2g} orbitals taking for the corresponding wave functions those of pure e_g and t_{2g} orbitals for cubic symmetry. However, trigonal distortion

can modify these wave functions, leading, in particular, to a mixing of e_g^σ and e_g^π orbitals. In this Appendix, we consider these effects; as a result, we find that their inclusion does not qualitatively modify our main conclusions, and can lead only to some change in certain numerical coefficients.

An elementary building block of transition metal compounds with face-sharing octahedra is shown in Fig. 2a. Magnetic atoms form a quasi-one-dimensional chain directed along the z axis. Each magnetic atom is surrounded by the distorted oxygen octahedron. Distortions are described by a single parameter θ , which is the angle between the z axis and the line connecting M and O atoms (see Fig. 2a). For undistorted octahedron, we have $\theta = \theta_0 = \arccos(1/\sqrt{3})$. The crystal field splits fivefold-degenerate d electron levels of the transition metal atom into two doubly degenerate e_g^σ , e_g^π levels, and a_{1g} level, as it is shown in Fig. 2b. The energy difference Δ_1 between e_g^π and a_{1g} levels can be positive or negative depending on the type of trigonal distortions. Stretching of oxygen octahedron ($\theta < \theta_0$) increases the energy of the a_{1g} level with respect to e_g^π one, leading to $\Delta_1 < 0$. However, the contribution to the crystal field from a neighboring magnetic cations acts in opposite direction, and, in general, we can have $\Delta_1 > 0$ even for (slightly) stretched octahedra.

Let us now discuss some details. In the point-charge approximation, the crystal field potential acting onto a chosen cation located at point \mathbf{r} can be represented as a sum of Coulomb terms

$$V(\mathbf{r}) = v_0 \sum_i \frac{r_0}{|\mathbf{r} - \mathbf{r}_i|}, \quad (\text{A1})$$

where \mathbf{r}_i are the positions of ligand ions. For d states, the existence of the threefold symmetry axis leads to a significant simplification of the expression for the crystal field, which can be, approximately, written in the following form

$$V(\mathbf{r}) = V_0(r) + v_1(r) \sum_{s=1}^3 P_2(\cos \theta_s) + v_2(r) \sum_{s=1}^3 P_4(\cos \theta_s), \quad (\text{A2})$$

where P_2 and P_4 are the Legendre polynomials, $P_2(x) = \frac{1}{2}(3x^2 - 1)$ and $P_4(x) = \frac{1}{8}(34x^4 - 30x^2 + 3)$. Here, we took into account the symmetry in the arrangement of two opposite edges of the ligand octahedron and as a result, we have

$$\cos \theta_s = \cos \theta' \cos \theta + \sin \theta' \sin \theta \cos \left(\phi' - \frac{2\pi s}{3} \right), \quad (\text{A3})$$

where θ' and ϕ' describe the direction of \mathbf{r} , that is, $\mathbf{r} = r\{\sin \theta' \cos \phi', \sin \theta' \sin \phi', \cos \theta'\}$.

Now, we should find the matrix elements of the crystal

field for the complete set of d functions

$$\begin{aligned}
 |xy\rangle &= R_d(r) \frac{\sin^2 \theta' \sin 2\phi'}{2}, \\
 |xz\rangle &= R_d(r) \sin \theta' \cos \theta' \cos \phi', \\
 |yz\rangle &= R_d(r) \sin \theta' \cos \theta' \sin \phi', \quad (\text{A4}) \\
 |x^2 - y^2\rangle &= R_d(r) \frac{\sin^2 \theta' \cos 2\phi'}{2}, \\
 |2z^2 - x^2 - y^2\rangle &= R_d(r) \frac{3 \cos^2 \theta' - 1}{2}.
 \end{aligned}$$

Straightforward, but rather cumbersome calculations, lead us to the following matrix

$$\hat{V}_{\alpha\beta} = E_0 \times \begin{pmatrix} \frac{-3a_4-10a_2}{15} & 0 & \frac{-b}{2} & 0 & 0 \\ 0 & \frac{12a_4+5a_2}{15} & 0 & \frac{b}{2} & 0 \\ \frac{-b}{2} & 0 & \frac{12a_4+5a_2}{15} & 0 & 0 \\ 0 & \frac{b}{2} & 0 & \frac{-3a_4-10a_2}{15} & 0 \\ 0 & 0 & 0 & 0 & \frac{-18a_4+10a_2}{15} \end{pmatrix},$$

where $E_0 = 10Dq$ is the splitting between e_g and t_{2g} levels, and

$$\begin{aligned}
 a_4 &= -\frac{3}{2} \left(\frac{5}{2} \cos^4 \theta - \frac{15}{7} \cos^2 \theta + \frac{3}{14} \right), \\
 a_2 &= \frac{27}{35} \kappa (3 \cos^2 \theta - 1), \\
 b &= 3 \sin^3 \theta \cos \theta.
 \end{aligned} \quad (\text{A5})$$

Here, parameter κ is defined as

$$\kappa = r_0^2 \frac{\int_0^\infty r^2 R_d^2(r) r^2 dr}{\int_0^\infty r^4 R_d^2(r) r^2 dr} = r_0^2 \frac{\langle r^2 \rangle}{\langle r^4 \rangle} = k \left(\frac{r_0}{a_B} \right)^2, \quad (\text{A6})$$

where r_0 is the cation–ligand distance and a_B is the Bohr radius. A rough estimate for the factor k can be found by using the hydrogen-like form for the radial part $R_d(r)$ of the wave function in metal ions, $R_d(r) \sim r^{n^*-1} \exp(-z^*r/a_B)$, where n^* and z^* , are the effective values of the principal quantum number and of the nuclear charge, respectively.⁴⁸ According to Ref. 48, we have $n^* = 3, 3.7$, and 4 for $3d, 4d$, and $5d$ shells, respectively. For d electrons, there is the following simple rule: the charge of all filled shells inside the d shell is subtracted from the nuclear charge and the charge of all d electrons except the given one is multiplied by 0.35 and also subtracted. For example, for Co^{4+} with the nuclear charge $z = 27$, we find $z^* = 7.6$. In this case, we have $k = (z^*)^2/810 \approx 0.07$. More accurate estimates using the linearized muffin-tin orbitals (LMTO) give $k = 0.2 - 0.3$.

As a result, we find the wave functions of e_g^σ, e_g^π , and a_{1g} energy levels, which depend on the trigonal distortions. Choosing the reference frame like shown in Fig. 2a, we obtain for the wave functions expressions having the forms similar to those obtained above for the case of

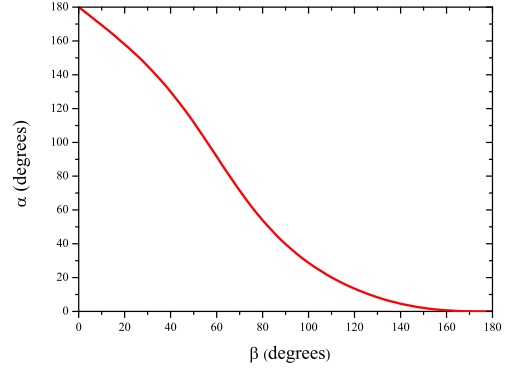


FIG. 3: (Color online) Angle α versus M1–O–M2 angle $\beta = \pi - 2\theta$; $k = 0.1$, $r_0 = 2 \text{ \AA}$.

undistorted octahedra. Thus, for e_g levels (e_g^σ orbitals) we have [cf. Eqs. (4) and (5)]

$$\begin{aligned}
 |d_{1,2}\rangle &= \sin \frac{\alpha}{2} |x^2 - y^2\rangle \mp \cos \frac{\alpha}{2} |xz\rangle, \\
 |e_{1,2}\rangle &= -\sin \frac{\alpha}{2} |xy\rangle \mp \cos \frac{\alpha}{2} |yz\rangle. \quad (\text{A7})
 \end{aligned}$$

For t_{2g} orbitals, we have the same a_{1g} singlet, Eqs. (16) and (18), and the e_g^π doublet [cf. Eqs. (17)–(19)]

$$\begin{aligned}
 |b_{1,2}\rangle &= -\cos \frac{\alpha}{2} |xy\rangle \pm \sin \frac{\alpha}{2} |yz\rangle, \\
 |c_{1,2}\rangle &= \cos \frac{\alpha}{2} |x^2 - y^2\rangle \pm \sin \frac{\alpha}{2} |xz\rangle. \quad (\text{A8})
 \end{aligned}$$

The \mp and \pm signs in the above expressions for cation wave functions for neighboring M atoms occur since the oxygen octahedra surrounding neighboring metal atoms are transformed to each other by the 180° rotation about z axis. Parameter α in Eqs. (A7) and (A8) depends on the trigonal distortions as well on the contribution to the crystal field from magnetic atoms. Neglecting the latter effect, we find

$$\cos \alpha = \frac{a}{\sqrt{a^2 + b^2}}, \quad a = a_2 + a_4. \quad (\text{A9})$$

For the ideal octahedron, we have $\alpha = \alpha_0 \equiv \pi - 2\theta_0 = \arccos(1/3)$. Substituting this value to Eqs. (A7) and (A8), we arrive at the results of the previous sections. The dependence of α on the M1–O–M2 angle $\beta = \pi - 2\theta$ is illustrated in Fig. 3. Parameter α decreases monotonically when β increases, and it changes faster for β close to the value $\beta_0 = \pi - 2\theta_0$ corresponding to the ideal octahedron. This decrease becomes sharper for larger values of κ .

These results were obtained neglecting the effect of neighboring metal atoms in the chain. Taking into account the contribution to the crystal field from these atoms modifies the parameter a_2 in the following manner

$$a_2 \rightarrow a_2 - \frac{27\kappa}{35} \frac{Z^*}{12 \cos^2 \theta}, \quad (\text{A10})$$

where Z^* is the effective charge (in units of e) of the metal ion. Note that Z^* can be different from z^* mentioned above. Parameters a_4 and b , as well as the relations (A7)–(A9) remain the same. Stretching of oxygen octahedra ($\theta < \theta_0$) tends to make $\alpha < \alpha_0$, while the effect of neighboring metal atoms acts in the opposite direction. For $\alpha > \alpha_0$, the energy of the a_{1g} level is lower than that of the e_g^π one (see Fig. 2b), leading to $\Delta_1 > 0$. Thus, in general, we can have $\Delta_1 > 0$ even for (slightly) stretched octahedra. Just this situation takes place in BaCoO₃ with the chains of face-sharing Co⁴⁺O₆ octahedra.²⁵ Here, Co⁴⁺ with the d^5 configuration has one hole at the e_g^π level.

The wave functions (A7) and (A8) are the generalization of those considered in the Sec. III–IV to the case of arbitrary trigonal distortion characterized by an angle α . In other words, these distortions mix the e_g^π and e_g^σ wave functions for ideal octahedra MO₆ given in Eqs. (4) and (5) and Eqs. (17)–(19).

It is quite straightforward to demonstrate that orbitals (A7) and (A8) provide the structure of the spin–orbital Hamiltonian of the same form of Eq. (14) at any given α (taking into account both direct and ligand-assistant hoppings). Thus, our main conclusions remain the same even with the $e_g^\sigma - e_g^\pi$ mixing taken into account.

Appendix B: Electron hopping via ligands

Here, we analyze a possible dependence of the hopping integrals between metal ions via ligand ions (let them call oxygens for brevity) on the M–O–M bond angle. In the chain of face sharing MO₆ octahedra, we chose a unit cell consisting of two oxygen triangles forming an octahedron and two metal ions, M1 and M2 (see Fig. 2). Then, the tight-binding Hamiltonian describing the charge transfer between metal ions via oxygen can be written in the following form (spin indices are omitted for simplicity)

$$H_{pd} = - \sum_{n\mu A} \left[t_{1\mu;1A} d_{n1\mu}^\dagger p_{n1A} + t_{2\mu;1A} d_{n2\mu}^\dagger p_{n1A} + t_{1\mu;2A} d_{n1\mu}^\dagger p_{n2A} + t_{2\mu;2A} d_{n2\mu}^\dagger p_{n-12A} + H.c. \right] + \Delta \sum_{nA} \left(p_{n1A}^\dagger p_{n1A} + p_{n2A}^\dagger p_{n2A} \right), \quad (\text{B1})$$

where n enumerates unit cells, $p^\dagger(p)$ and $d^\dagger(d)$ are creation (annihilation) operators for p and d electrons, respectively, numbers 1 and 2 correspond to metal ions M1 and M2, respectively, and to the oxygen triangle above each of them, μ is the set of basis d functions [Eqs. (A7) for e_g^σ orbitals or Eqs. (A8) for e_g^π orbitals], and $A = \{s, \eta\}$, where $s = 1, 2, 3$ and $\eta = p_x, p_y, p_z$, is a set of subscripts numbering the atoms in each oxygen triangle and denoting the oxygen p orbitals. For each doublet (e_g^σ or e_g^π), we have four $d_{nl\mu}$ ($l = 1, 2$) operators and eighteen p_{njA} ($j = 1, 2$) operators, for which we should take into account all possible electron hoppings.

In the second order of the perturbation theory on t_{pd}/Δ , we can derive a Hamiltonian describing the effective hoppings of electrons between the states of d doublets under study via the oxygen p orbitals. To do this, we first proceed to the momentum representation for electronic operators $d_{kl\mu} = \sum_n e^{-2ikz_0 n} d_{nl\mu} / \sqrt{N}$, $p_{kjA} = \sum_n e^{-2ikz_0 n} p_{njA} / \sqrt{N}$, where N is the number of unit cells in the chain and $z_0 = 2r_0 \cos \theta$ is the distance between neighboring M1 and M2 atoms (r is the M–O distance). Following then the standard procedure, we obtain for the effective Hamiltonian

$$H_{eff} = - \sum_{k\mu\nu} \left[t_{\mu\nu}(k) d_{k1\mu}^\dagger d_{k2\nu} + H.c. \right], \quad (\text{B2})$$

where ($t_{l\mu;jA}$ are assumed to be real)

$$t_{\mu\nu}(k) = \frac{1}{\Delta} \sum_A \left[t_{1\mu;1A} t_{2\nu;1A} + t_{1\mu;2A} t_{2\nu;2A} e^{-ikz_0} \right]. \quad (\text{B3})$$

According to Ref. 46, the hopping amplitudes $t_{l\mu;jA}$ can be expressed via two Slater–Koster parameters $V_{pd\sigma}$ and $V_{pd\pi}$ and directing cosines of the radius vector \mathbf{r} connecting the corresponding oxygen and metal ions⁴⁹. If we choose the reference frame as shown in Fig. 2, the radius vector $\mathbf{r}_{l;js}$ directed from the oxygen atom $s(=1, 2, 3)$ in the j th ($j = 1, 2$) group of oxygens to the neighboring metal ion $l(l=1, 2)$ is

$$\mathbf{r}_{l;js} = r_0 (-1)^j \{ \sin \theta \cos \varphi_s, \sin \theta \sin \varphi_s, (-1)^{l-1} \cos \theta \}, \quad (\text{B4})$$

where $\varphi_s = 2\pi(s-1)/3$. Using these relations, Table I of Ref. 46, and Eqs. (A7) for e_g^σ orbitals or Eqs. (A8) for e_g^π orbitals, we calculate the hopping amplitudes $t_{l\mu;jA}$ as functions of Slater–Koster parameters $V_{pd\sigma}$ and $V_{pd\pi}$, the angle θ , and the parameter α describing the orbital states. Substituting then the obtained $t_{l\mu;jA}$ into Eq. (B3) and performing the summation, we arrive finally to the following relation for the effective d – d hopping amplitudes

$$t_{\mu\nu}(k) = \delta_{\mu\nu} t_0 (1 + e^{-ikz_0}). \quad (\text{B5})$$

This relation is valid both for e_g^σ and e_g^π orbitals. For e_g^σ orbitals, the parameter t_0 is

$$t_0 = -\frac{9}{8} \frac{V_{pd\sigma}^2}{\Delta} \sin^2 \theta \cos 2\theta \left(2 \cos \theta \cos \frac{\alpha}{2} - \sin \theta \sin \frac{\alpha}{2} \right)^2 + \frac{3}{2} \frac{V_{pd\pi}^2}{\Delta} \left[\left(\sin \theta \sin \frac{\alpha}{2} + \cos \theta \cos \frac{\alpha}{2} \right)^2 + \cos 2\theta \left(\sin \theta \cos \theta \sin \frac{\alpha}{2} - \cos 2\theta \cos \frac{\alpha}{2} \right)^2 \right] + \frac{3\sqrt{3}}{2} \frac{V_{pd\sigma} V_{pd\pi}}{\Delta} \sin \theta \sin 2\theta \left[\sin^2 \theta \cos \theta \sin^2 \frac{\alpha}{2} - \sin \theta (3 \cos^2 \theta - \sin^2 \theta) \sin \frac{\alpha}{2} \cos \frac{\alpha}{2} + 2 \cos \theta \cos 2\theta \cos^2 \frac{\alpha}{2} \right]. \quad (\text{B6})$$

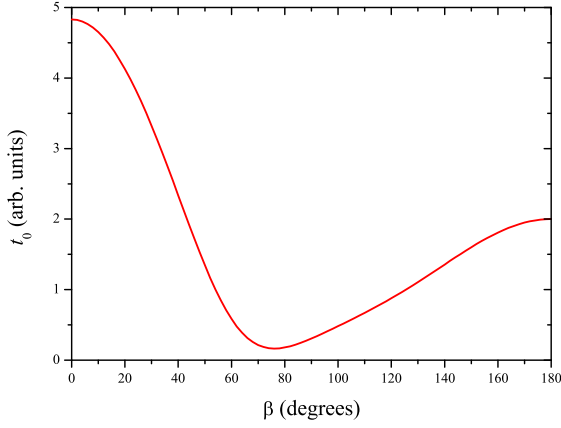


FIG. 4: (Color online) Hopping integral for e_g^σ orbitals versus M1-O-M2 angle $\beta = \pi - 2\theta$; $k = 0.1$, $r_0 = 2$ Å.

In the case of e_g^π electrons, the hopping integral t_0 reads

$$\begin{aligned}
 t_0 = & -\frac{9}{8} \frac{V_{pd\sigma}^2}{\Delta} \sin^2 \theta \cos 2\theta \left(2 \cos \theta \sin \frac{\alpha}{2} - \sin \theta \cos \frac{\alpha}{2} \right)^2 + \\
 & \frac{3}{2} \frac{V_{pd\pi}^2}{\Delta} \left[\left(\sin \theta \cos \frac{\alpha}{2} + \cos \theta \sin \frac{\alpha}{2} \right)^2 + \right. \\
 & \left. \cos 2\theta \left(\sin \theta \cos \theta \cos \frac{\alpha}{2} - \cos 2\theta \sin \frac{\alpha}{2} \right)^2 \right] + \\
 & \frac{3\sqrt{3}}{2} \frac{V_{pd\sigma} V_{pd\pi}}{\Delta} \sin \theta \sin 2\theta \left[\sin^2 \theta \cos \theta \cos^2 \frac{\alpha}{2} - \right. \\
 & \left. \sin \theta (3 \cos^2 \theta - \sin^2 \theta) \sin \frac{\alpha}{2} \cos \frac{\alpha}{2} + \right. \\
 & \left. 2 \cos \theta \cos 2\theta \sin^2 \frac{\alpha}{2} \right]. \quad (B7)
 \end{aligned}$$

Note, that the effective Hamiltonian (B2) with hopping amplitudes of the form of Eq. (B5) is equivalent to the simple tight-binding Hamiltonian of the form

$$H_{eff} = -t_0 \sum_{m\mu} \left[d_{m\mu}^\dagger d_{m+1\mu} + H.c. \right]. \quad (B8)$$

This can be easily checked by using the transformation for electronic operators

$$d_{n1\mu} \rightarrow d_{2m\mu}, \quad d_{n2\mu} \rightarrow d_{2m+1\mu}, \quad m \in \mathbb{Z}. \quad (B9)$$

Thus, from viewpoint of the electronic properties, the magnetic sites M1 and M2 are equivalent to each other even though crystallographically they are different. One should keep in mind, however, that d -orbitals wave functions of neighboring magnetic sites are different.

The dependence of the hopping integral t_0 for e_g^σ and e_g^π orbitals on the M-O-M bond angle $\beta = \pi - 2\theta$ is illustrated in Figs. 4 and 5, respectively. For the ratio $V_{pd\sigma}/V_{pd\pi}$, we took the commonly used value⁵⁰ equal to 2.16. We see that at some value of β the hopping integral via oxygens either changes sign (for e_g^π orbitals) or becomes close to zero (for e_g^σ orbitals).

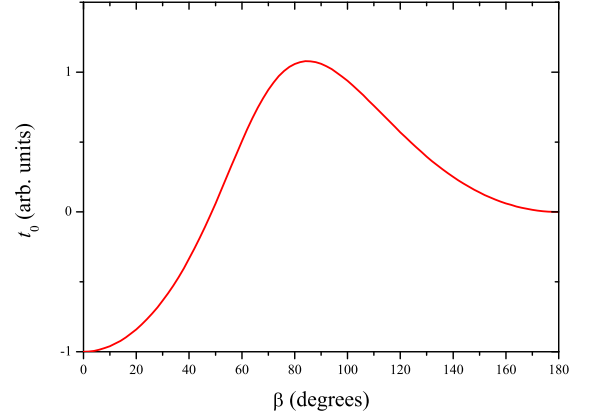


FIG. 5: (Color online) Hopping integral for e_g^π orbitals versus M1-O-M2 angle $\beta = \pi - 2\theta$; $k = 0.1$, $r_0 = 2$ Å.

For e_g^σ orbitals this happens for M-O-M bond angle close to that characteristic of an undistorted octahedron $\beta_0 = \pi - 2 \arccos(1/\sqrt{3}) \cong 70.5^\circ$, while for e_g^π orbitals t_0 changes the sign at a bit smaller value of β (compressed octahedron). The total d - d hopping amplitude is $t = t_0 + t^{d-d}$. Thus, for e_g^σ orbitals t is always positive, while for e_g^π orbitals it can change sign. Usually, the direct d - d hopping amplitude t^{d-d} is assumed to be smaller than the characteristic value of the effective hopping via oxygens $t_0 \sim V_{pd\sigma}^2/\Delta$. Our calculations show however, that for some M-O-M bond angles the direct hopping becomes dominant. Moreover, for e_g^σ orbitals this can be the case of the ideal octahedron. When the hopping is suppressed, the higher-order corrections to the SU(4) model, containing the terms $\sim J/U$, which have less symmetric form in orbital τ variables (see e.g. Refs. 4 and 5) may have to be included.

Appendix C: General form of the exchange Hamiltonian

Let us now present the full form of the exchange Hamiltonian, including terms containing the Hund's rule coupling constant J . These terms appear when we consider not the virtual hopping between occupied orbitals, but the hopping to an empty orbital of the neighbor, with the consecutive effect of Hund's coupling. The derivation of these terms is straightforward^{4,5}, although a bit cumbersome. In our case of face-sharing octahedra, the resulting spin-orbital Hamiltonian has the form

$$\begin{aligned}
 H_{eff} = & \frac{t^2}{U} \sum_{\langle i,j \rangle} \left\{ \left(\frac{1}{2} + 2\mathbf{s}_i \mathbf{s}_j \right) \left(\frac{1}{2} + 2\boldsymbol{\tau}_i \boldsymbol{\tau}_j \right) + \right. \quad (C1) \\
 & \frac{JU}{U^2 - J^2} [2(\boldsymbol{\tau}_i \boldsymbol{\tau}_j - \tau_i^z \tau_j^z) - \left(\frac{1}{2} + 2\mathbf{s}_i \mathbf{s}_j \right) \left(\frac{1}{2} - 2\tau_i^z \tau_j^z \right)] + \\
 & \left. \frac{J^2}{U^2 - J^2} \left[(2\tau_i^z \tau_j^z - \frac{1}{2}) + (1 + 2\mathbf{s}_i \mathbf{s}_j) (\boldsymbol{\tau}_i \boldsymbol{\tau}_j - \tau_i^z \tau_j^z) \right] \right\}.
 \end{aligned}$$

We see indeed that, whereas the leading term in the full

Hamiltonian (C1) has the $SU(4)$ form, its symmetry is broken by the terms of higher order in J/U . Nevertheless, for many realistic situations these terms give only a small correction to the main term, which could in principle be smaller than the results of quantum fluctuations in the $SU(4)$ model. And, as mentioned above, even if these

symmetry-breaking terms would determine the type of the ordering in the ground state at $T = 0$, there would exist a broad temperature range $(t^2/U)(J/U) \lesssim T \lesssim t^2/U$, in which the properties of the system would be determined by the first, $SU(4)$, part of the Hamiltonian.

-
- ¹ J.B. Goodenough, *Magnetism and the Chemical Bond* (Wiley Interscience, New York, 1963).
 - ² D.I. Khomskii, *Transition Metal Compounds* (Cambridge University Press, Cambridge, 2014).
 - ³ A. M. Oleś, J. Phys.: Condens. Matter **24**, 313201 (2012).
 - ⁴ K.I. Kugel and D.I. Khomskii, Zh. Eksp. Teor. Fiz. **64**, 1429 (1973) [JETP **37**, 725 (1973)].
 - ⁵ K.I. Kugel and D.I. Khomskii, Usp. Fiz. Nauk **136**, 621 (1982) [Sov. Phys.-Uspekhi **25**, 231 (1982)].
 - ⁶ Z. Nussinov and J. van den Brink, Rev. Mod. Phys. **87**, 1 (2015).
 - ⁷ A. Kitaev, Ann. Phys. (N. Y). **321**, 2 (2006).
 - ⁸ D.I. Khomskii, Phys. Scripta **72**, CC8 (2005).
 - ⁹ S.K. Pati, R.R.P. Singh, and D.I. Khomskii, Phys. Rev. Lett. **81**, 5406 (1998).
 - ¹⁰ B. Sutherland, Phys. Rev. B **12**, 3795 (1975).
 - ¹¹ B. Frischmuth, F. Mila, and M. Troyer, Phys. Rev. Lett. **82**, 835 (1999).
 - ¹² G.-M. Zhang, H. Hu, and L. Yu, Phys. Rev. B **67**, 064420 (2003).
 - ¹³ Y.Q. Li, M. Ma, D.N. Shi, and F.C. Zhang, Phys. Rev. Lett. **81**, 3527 (1998).
 - ¹⁴ M. van den Bossche, P. Azaria, P. Lecheminant, and F. Mila, Phys. Rev. Lett. **86**, 4124 (2001).
 - ¹⁵ P. Corboz, A.M. Läuchli, K. Penc, M. Troyer, and F. Mila, Phys. Rev. Lett. **107**, 215301 (2011).
 - ¹⁶ P. Corboz, M. Lajkó, A.M. Läuchli, K. Penc, and F. Mila, Phys. Rev. X **2**, 041013 (2012).
 - ¹⁷ K. Penc, M. Mambrini, P. Fazekas, and F. Mila, Phys. Rev. B **68**, 012408 (2003).
 - ¹⁸ F. Vernay, K. Penc, P. Fazekas, and F. Mila, Phys. Rev. B **70**, 014428 (2004).
 - ¹⁹ A. Smerald and F. Mila, Phys. Rev. B **90**, 094422 (2014).
 - ²⁰ A.V. Gorshkov, M. Hermele, V. Gurarie, C. Xu, P.S. Julienne, J. Ye, P. Zoller, E. Demler, M.D. Lukin, and A.M. Rey, Nature Phys. **6**, 289 (2010).
 - ²¹ M.V. Mostovoy and D.I. Khomskii, Phys. Rev. Lett. **89**, 227203 (2002).
 - ²² D.I. Khomskii and M.V. Mostovoy, J. Phys. A: Mat. and Gen. **36**, 9197 (2003).
 - ²³ J. van den Brink and D. Khomskii, Phys. Rev. B **63**, 140416(R) (2001).
 - ²⁴ S.V. Streltsov and D.I. Khomskii, Phys. Rev. B **77**, 064405 (2008).
 - ²⁵ K. Yamaura, H.W. Zandbergen, K. Abe, and R.J. Cava, J. Solid State Chem. **146**, 96 (1999).
 - ²⁶ R.A. Gardner, M. Vlasse, and A. Wold, Acta Cryst. **B25**, 781 (1969).
 - ²⁷ S. Hirotsu, J. Phys. C: Solid State Phys. **10**, 967 (1977).
 - ²⁸ T. Siegrist and B.L. Chamberland, J. Less-Common Metals **170**, 93 (1991).
 - ²⁹ S.-T. Hong and A.W. Sleight, J. Solid State Chem. **128**, 251 (1997).
 - ³⁰ J.G. Zhao, L.X. Yang, Y. Yu, F.Y. Li, R.C. Yu, Z. Fang, L.C. Chen, and C.Q. Jin, J. Solid State Chem. **180**, 2816 (2007).
 - ³¹ A.H. Carim, P. Dera, L.W. Finger, B. Mysen, C.T. Prewitt, and D.G. Schlom, J. Solid State Chem. **149**, 137 (2000).
 - ³² Y. Klein, G. Rousse, F. Damay, F. Porcher, G. André, and I. Terasaki, Phys. Rev. B **84**, 054439 (2011).
 - ³³ P. Köhl and D. Reinen, Z. anorg. allg. Chem. **433**, 81 (1977).
 - ³⁴ S.A.J. Kimber, M.S. Senn, S. Fratini, H. Wu, A.H. Hill, P. Manuel, J.P. Attfield, D.N. Argyriou, and P.F. Henry, Phys. Rev. Lett. **108**, 217205 (2012).
 - ³⁵ M.S. Senn, A.M. Arevalo Lopez, T. Saito, Y. Shimakawa, and J. Paul Attfield, J. Phys.: Condens. Matter **25**, 496008 (2013).
 - ³⁶ I. Fernandez, R. Greatrex, and N.N. Greenwood, J. Solid State Chem. **34**, 121 (1980).
 - ³⁷ M.S. Senn, S.A.J. Kimber, A.M. Arevalo Lopez, A.H. Hill, and J.P. Attfield, Phys. Rev. B **87**, 134402 (2013).
 - ³⁸ J.T. Rijssenbeek, Q. Huang, R.W. Erwin, H.W. Zandbergen, and R.J. Cava, J. Solid State Chem. **146**, 65 (1999).
 - ³⁹ J.T. Rijssenbeek, R. Jin, Y. Zadorozhny, Y. Liu, B. Batlogg, and R.J. Cava, Phys. Rev. B **59**, 4561 (1999).
 - ⁴⁰ S.V. Streltsov, Phys. Rev. B **88**, 024429 (2013).
 - ⁴¹ U. von Treiber, S. Kemmler-Sack, and A. Ehmann, Z. anorg. allg. Chem. **487**, 189 (1982).
 - ⁴² S.V. Streltsov and D.I. Khomskii, Phys. Rev. B **86**, 064429 (2012).
 - ⁴³ P. Lightfoot and P.D. Battle, J. Solid State Chem. **89**, 174 (1990).
 - ⁴⁴ A. Abragam and B. Bleaney, *Electron Paramagnetic Resonance of Transition Ions* (Clarendon Press, Oxford, 1970).
 - ⁴⁵ C.A. Bates, P.E. Chandler, and K.W.H. Stevens, J. Phys. C: Solid State Phys. **4**, 2017 (1971).
 - ⁴⁶ J.C. Slater and G.F. Koster, Phys. Rev. **94**, 1498 (1954).
 - ⁴⁷ I.B. Bersuker, *The Jahn-Teller Effect* (Cambridge University Press, Cambridge, 2006).
 - ⁴⁸ J.C. Slater, Phys. Rev. **36**, 57 (1930).
 - ⁴⁹ These cosines are usually (and in Ref. 46) denoted as l , m , and n , that is, for the radius vector \mathbf{r} , we have $\mathbf{r} \equiv r\{l, m, n\}$.
 - ⁵⁰ W.A. Harrison, *Electronic Structure and the Properties of Solids* (Dover, Mineola, NY, 1989).